An Isotope-Edited FT-IR Study of a Symporter, the Lactose Permease†

Jason S. Patzlaff,‡,§ Jingyan Zhang,‡,|| Robert J. Brooker,|| and Bridgette A. Barry*,‡

Department of Biochemistry, Molecular Biology, and Biophysics and Department of Genetics, Cell Biology, and Development and the Biotechnology Institute, University of Minnesota, St. Paul, Minnesota 55108

Received January 15, 2002; Revised Manuscript Received April 9, 2002

ABSTRACT: The lactose permease of *Escherichia coli* transports protons and lactose across the plasma membrane and uses a transmembrane ion gradient as the energy source to drive the uphill accumulation of lactose. In this report, the effect of the electrochemical gradient on the permease has been studied. Bacteriorhodopsin was co-reconstituted with the lactose permease to provide a light-triggered electrochemical gradient. Reaction-induced Fourier transform infrared spectra were acquired, and bacteriorhodopsin contributions were subtracted. In previous work, positive bands in the 1765−1730 cm^{-1} region of the reaction-induced FT-IR spectrum were attributed to the perturbation of carboxylic acid residues in the permease [Patzlaff, J. S., Brooker, R. J., and Barry, B. A. (2000) *J. Biol. Chem. 275*, 28695−28700]. In this study, we have globally labeled the permease with ^{13}C or ^{15}N. Isotopic labeling demonstrates that features in the reaction-induced FT-IR spectrum arise from permease carboxylic acid, amide I, and amide II vibrational modes. In addition, isotope labeling leads to a tentative assignment of spectral features to lysine, arginine, histidine, glutamine, and/or asparagine in the permease. These results indicate that the electrochemical gradient causes changes in the environment or protonation state of carboxylic acid residues in the permease and suggest an interaction between these carboxylic acid side chains and nitrogen-containing amino acid side chains. Evidence for a change in secondary structure, corresponding to an interconversion of secondary structural elements, a change in the hydrogen-bonding strength, or coupling of peptide vibrational modes, is also presented. These experiments demonstrate the usefulness of reaction-induced spectroscopy in the study of transmembrane transport.

The lactose permease is an inducible system for the accumulation of galactosides in *Escherichia coli* (*1*). The membrane protein is a member of the major facilitator superfamily (MFS);[1] members of the MFS catalyze uniport, symport, or antiport (*2*). Lactose permease has been studied as a model for symport processes. The basic function of this protein is the symport of protons and β-galactosides at a 1 to 1 ratio. The free energy stored in a gradient of either protons or β-galactosides can be used to accumulate the symport partner against a concentration gradient (*3*).

The permease is encoded by the *lacY* gene, and the gene has been cloned into recombinant plasmids and sequenced (*4*, *5*). These studies show that the permease contains 417 amino acid residues and predict the molecular mass to be 46.5 kDa (*5*). A secondary structural model of 12 α-helical transmembrane spanning domains has been proposed and supported by circular dichroism, FT-IR spectroscopy, antibody binding, limited proteolysis, and permease−alkaline phosphatase fusion assays (*6*−*10*). The protein has also been characterized by cysteine-scanning mutagenesis studies, and it has been shown that only a few amino acid residues are critical for structure/function (reviewed in refs *11* and *12*). Eight amino acid residues, all of which are charged and predicted to lie within transmembrane regions, were shown to play a critical role. Subsequently, these amino acid residues have been the focus of attention, and it has been postulated that these residues provide proton and/or lactose binding sites (reviewed in refs *11* and *12*). For example, a negatively charged residue, E325, has been proposed to be a site of proton binding (*13*, *14*). However, double and triple mutagenesis studies suggest that alternate proton binding sites may exist or that hydronium ion is the transported species (*15*, *16*).

Recently, new experimental methods have been used to gather detailed information concerning the permease. These studies include the use of biophysical techniques, such as spin labeling and EPR spectroscopy, to determine the distance between selected amino acid residues (*17*). Fluorescent labeling assays have been employed to probe helical arrangement (see, for example, refs *18* and *19*). Fourier transform infrared spectroscopic studies have been performed to assay secondary structure and solvent accessibility (*9*, *10*). These studies have been valuable in modeling the secondary and tertiary structure of the lactose permease.

In our recent work, we have extended these biophysical studies with the goal of obtaining dynamic information about the permease as it responds to a H^+ electrochemical gradient

† Supported by NIH Grant GM 53259.

* Address correspondence to this author. Phone: 612-624-6732. Fax: 612-625-5780. E-mail: barry@biosci.cbs.umn.edu.

‡ Department of Biochemistry, Molecular Biology, and Biophysics, University of Minnesota.

§ Current address: Department of Biochemistry, Groningen Biomolecular Sciences and Biotechnology Institute, University of Groningen, Nijenborgh 4, 9747 AG Groningen, The Netherlands.

|| Department of Genetics, Cell Biology, and Development and the Biotechnology Institute, University of Minnesota.

[1] Abbreviations: Δ*A*, change in absorbance; FT-IR, Fourier transform infrared; MFS, major facilitator superfamily.

10.1021/bi025555g CCC: $22.00
Published on Web 05/16/2002

(*20*). Reaction-induced difference Fourier transform infrared spectroscopy was used to study liposomes containing both the permease and the light-driven proton pump, bacteriorhodopsin. This system allowed us to obtain reaction-induced FT-IR spectra on a single sample as it was modulated between two states: a light-induced state in which the electrochemical gradient had been imposed across the membrane and a dark-adapted state in which the gradient had dissipated. Bacteriorhodopsin spectral features were subtracted to yield a spectrum that reflected structural changes in the lactose permease. This analysis led to the identification of spectral features, which were attributed to electrochemical gradient-induced structural changes in the permease. In this previous study, we tentatively attributed vibrational bands in the 1760−1730 cm^{-1} region to carboxylic acid residues in the lactose permease (*20*). We speculated that these carboxylic acid residues were perturbed by the gradient through changes in pK_a, protonation state, or environment.

In this report, the permease has been globally labeled with ^{13}C or ^{15}N. Global labeling was accomplished by growing permease-expressing *E. coli* strains on a ^{13}C-enriched carbon source or a ^{15}N-enriched nitrogen source. In spectra acquired on both samples, isotope-induced downshifts were observed in permease vibrational lines. These isotope shifts identify permease vibrational modes involving carbon and nitrogen displacements, respectively. We compare the ^{13}C- and ^{15}N-induced isotope shifts to propose an initial set of assignments for permease vibrational bands. Permease contributions were also monitored as a function of time after photoexcitation and were observed to decay with the dissipation of the electrochemical gradient.

MATERIALS AND METHODS

Lactose Permease Purification. A histidine-tagged construct of the lactose permease was purified from *E. coli* cell membranes by methods previously described (*10*). For these labeling studies, cells were grown in minimal media containing either [^{12}C]glucose or [^{13}C]glucose (Isotech Labs, 98% ^{13}C globally labeled glucose) as the sole carbon source. Fifty milliliter starter cultures of minimal media containing 1.5% [^{13}C]- or [^{12}C]glucose were inoculated from 1 mL glycerol stocks. These starter cultures were then used to inoculate 1 L cultures of minimal media containing 1.5% [^{13}C]- or [^{12}C]-glucose. This serial dilution minimized potential ^{12}C carryover from the glycerol inoculum. For isolation of ^{15}N-labeled lactose permease, cells were grown in minimal media containing $^{15}NH_4Cl$ (Cambridge Isotopes, 99% ^{15}N labeled). Once purified, the lactose permease was mixed with sonicated, acetone/ether-washed *E. coli* lipids and reconstituted by a previously described dialysis method (*10*). The lipid to permease molar ratio was 520:1.

Analysis of Permease Isotopic Composition. Purified lactose permease was analyzed to determine the level of ^{13}C incorporation, as previously described (*21*). The protein was washed in water three times to remove salts and buffer components and subjected to acid hydrolysis. The acid-hydrolyzed amino acids of the lactose permease were derivatized with a *tert*-butyldimethylsilyl group (*22*). This reagent makes the sample volatile for gas chromatography. The derivatized amino acids were subjected to gas chromatography/mass spectrometry using a Kratos MS-25 GC/MS equipped with a DB-1 column (J&W Scientific, Folsom, CA). The derivatized amino acids were identified by their elution time, and the mass/charge ratio was determined. The percentage of uniform ^{13}C labeling was assessed for individual amino acids and was found to be 87% (*21*). An additional small percentage (∼7%) was enriched for ^{13}C at one or more carbon atoms but was also determined and was not uniformly ^{13}C labeled. The percentage of uniform ^{15}N labeling was determined and was >95%.

Bacteriorhodopsin Purification. Purple membranes were isolated from *Halobacterium halobium* using previously described techniques (*20*). Briefly, crude purple membranes were obtained from cells that had been lysed in water containing DNase. A series of water washes and high-speed centrifugation enriched for the purple membrane fraction. Sedimentation of the crude purple membranes through a 5−40% sucrose gradient (18 h) provided the final purification step. The purple band was removed from the gradient and washed to remove the sucrose. The resulting A_{568}/A_{280} ratio was 0.45−0.57.

Co-reconstitution of Bacteriorhodopsin and the Lactose Permease. Bacteriorhodopsin and lactose permease were co-reconstituted as previously described (*20*). Bacteriorhodopsin and lactose permease were mixed at a 1.6:1.0 molar ratio and frozen rapidly in liquid nitrogen. This mixture was then removed from liquid nitrogen and allowed to thaw slowly at room temperature. Three cycles of freeze/thaw were performed, and the final sample was frozen for storage at −80 °C. As the control, a bacteriorhodopsin sample was mixed with sonicated, acetone/ether-washed *E. coli* lipids without permease and subjected to the same freeze/thaw procedure. Our previous work on this type of liposome has shown light-induced changes in permease counterflow assays, consistent with successful co-reconstitution (*20*).

FT-IR Spectroscopy. Reaction-induced FT-IR spectra were acquired through the use of a Nicolet 60SXR spectrometer as described previously (*20*). The mirror velocity was 1.57 cm s^{-1}; the spectral resolution was 8 cm^{-1}, and 360 mirror scans (or 1 min of data collection) were co-added for each single-sided interferogram. A Happ−Genzel apodization function and one level of zero filling were employed. The proteoliposome sample was positioned onto a 25 mm CaF_2 window and partially dehydrated under a stream of N_2 gas at 4 °C. The final amide II absorbance for each sample was between 0.2 and 0.5 absorbance unit.

As an independent measure of the concentrations of bacteriorhodopsin and lactose permease, UV−visible spectra were recorded of each FT-IR sample using a Hitachi Model U-3000 (Tokyo, Japan) spectrophotometer. A clean CaF_2 window was used as a blank. The sample was then sandwiched between a germanium window and was placed into a Harrick temperature control FT-IR cell. The sample holder and temperature controller have been described previously (*20*). The sample temperature was allowed to equilibrate to 0 °C, and the sample compartment was purged with nitrogen for a minimum of 2 h to remove water vapor prior to sample data collection. Illumination was provided through the use of the 532 nm second harmonic of a pulsed laser (Surelight I, Continuum, Santa Clara, CA), and there was an approximate 0.7 s time delay before the beginning of the FT-IR data collection. Labview software (National

Instruments, Austin, TX) was used to initiate laser pulses and to trigger data collection. Bacteriorhodopsin was converted to the light-adapted form before data collection through 10 laser pulses (at 1 Hz illumination). Data collection began with a 1 min scan, and then the sample was given 5 laser pulses (1 Hz each). Data were then collected for five (1 min) data sets. This data collection cycle was performed 10−30 times (i.e., approximately 1−3 h of data collection).

Individual difference spectra were normalized and averaged. To compare the control with ^{13}C-labeled samples, the amide II amplitude, measured from the FT-IR absorption spectrum, was used to normalize the spectra. This normalization corrects for small differences in path length and/or protein concentration. The amide II band amplitude was used because there was a line shape change in the amide I band upon ^{13}C labeling of the permease. This line shape change was due to the downshift of the permease amide I band. To compare the control with ^{15}N-labeled samples, the amide I amplitude, measured from the FT-IR absorption spectrum, was used to normalize the spectra. This procedure was used because the frequency of the amide I band was found to be less sensitive to ^{15}N labeling, when compared to the amide II band. In each case, an additional correction for the concentration of bacteriorhodopsin and lactose permease was performed through the use of the 280 nm/565 nm ratio, which was recorded on each FT-IR sample. Double difference spectra, reflecting only the contributions of the lactose permease, were generated by subtracting a corrected bacteriorhodopsin difference spectrum (method I). Bacteriorhodopsin contributions were also eliminated by subtracting the ^{13}C-labeled lactose permease spectrum directly from the control or by subtracting the ^{15}N-labeled lactose permease spectrum directly from the control (method II). As shown below, these two bacteriorhodopsin subtraction methods gave similar results. The isotope-edited, double difference spectra, recorded on different samples, showed some overall amplitude variation, when different samples were compared. This amplitude variation may be due to a small contribution from permease proteoliposomes that do not contain bacteriorhodopsin. To average potential variations in permease content, many data sets were recorded on multiple samples. A total of 270 difference spectra were acquired from 9 control samples, 180 difference spectra were acquired from 6 ^{13}C samples, and 480 difference spectra were acquired from 16 ^{15}N samples.

RESULTS

To assign spectral features in the reaction-induced FT-IR spectrum, the permease was globally labeled with ^{13}C or ^{15}N, and co-reconstituted with bacteriorhodopsin. Dark-adapted samples were subjected to laser flashes, which activate bacteriorhodopsin and produce a H^+ electrochemical gradient. Subtraction of dark-adapted spectra from those obtained at four 60 s time intervals after the laser flash generates four reaction-induced FT-IR spectra. These spectra reflect the permease structural changes, which are induced by the H^+ electrochemical gradient. This procedure also permits these structural changes to be monitored as a function of time.

Figure 1 presents the reaction-induced FT-IR spectrum acquired in the first 60 s after the flash; bacteriorhodopsin was subtracted by method I (see Materials and Methods). In Figure 1A (dotted line), the permease was purified from *E. coli* cells grown on natural abundance ^{12}C/^{14}N carbon/nitrogen sources. As expected, the double difference spectrum is similar to the spectrum presented in our earlier study (*20*). As reported previously (*20*), the 1650 ± 10 cm^{-1} region showed significant variation from reconstituted sample to sample and so will not be considered further. The solid line in Figure 1A is the difference spectrum obtained with the ^{13}C-labeled permease. Vibrational modes that involve displacement of carbon are expected to downshift in frequency when ^{13}C is substituted for ^{12}C. As shown in Figure 1A (solid line), changes in amplitude and frequency were indeed observed upon isotopic substitution.

The changes that occur upon ^{13}C isotopic substitution are more easily seen when the ^{13}C spectrum (solid line, Figure 1A) is subtracted from the ^{12}C spectrum (Figure 1A, dotted line). The result (subtraction method I) is presented in Figure 1B. A significant ^{13}C-induced shift in vibrational bands in the 1740−1730 cm^{-1} region is observed. Alterations are also observed in the 1680−1660, 1640−1620, 1540−1520, and 1469 cm^{-1} regions. As revealed by comparison of the isotope-edited spectrum (Figure 1B) with the negative controls (Figure 1E,F), these spectral changes are significant and above the noise in the measurements.

Figure 1C, solid line, shows the difference spectrum acquired from the ^{15}N-labeled permease. Again, spectral changes were observed; these changes were consistent with ^{15}N-induced isotope shifts in permease bands. Subtraction by method I gave an isotope-edited spectrum in which these changes are apparent (Figure 1D). ^{15}N shifts were observed in the 1680−1660, 1640−1630, 1540−1520, and 1469 cm^{-1} regions (Figure 1D). Comparison of spectra C and D of Figure 1 reveals that ^{13}C and ^{15}N substitution have different effects on the spectrum. This is expected because ^{13}C and ^{15}N isotope-induced shifts are different in magnitude for most vibrational modes. Frequencies in common between the two isotope-edited spectra may arise from the ^{12}C/^{14}N band.

Apparent ^{15}N spectral changes in the 1750−1700 cm^{-1} region are intriguing (Figure 1D). In model compounds, nitrogen-containing amino acid side chains do not absorb in this spectral region (*23*, *24*). However, our ^{15}N isotope-edited spectrum may provide evidence for a substantial isotope shift of a negative 1758 cm^{-1} band to positive 1732 cm^{-1}; such an isotope shift is consistent with a spectral contribution from a nitrogen-containing amino acid side chain. Strong electrostatic interactions could be responsible for such a substantial shift of frequency, when the protein environment is compared to model compounds (*25*). However, given the signal to noise (compare Figure 1D with Figure 1E,F), these data must be corroborated by a study of site-directed mutants.

The 1760 cm^{-1} band does not exhibit a significant ^{13}C or ^{15}N shift upon permease labeling (Figure 1A,C). Therefore, it is unlikely that this is a permease band. A possible assignment is a lipid ester vibration, which is perturbed when the permease undergoes a conformational change. A perturbed lipid molecule would also contribute to other spectral regions. Because such a lipid perturbation would cancel out in the isotope-edited spectrum, such a contribution could account for the small magnitude of the isotope-edited spectra, relative to Figure 1A. Alternatively, a small error in bacteriorhodopsin subtraction could give a residual bacteriorhodopsin contribution in Figure 1A. A discussion of this

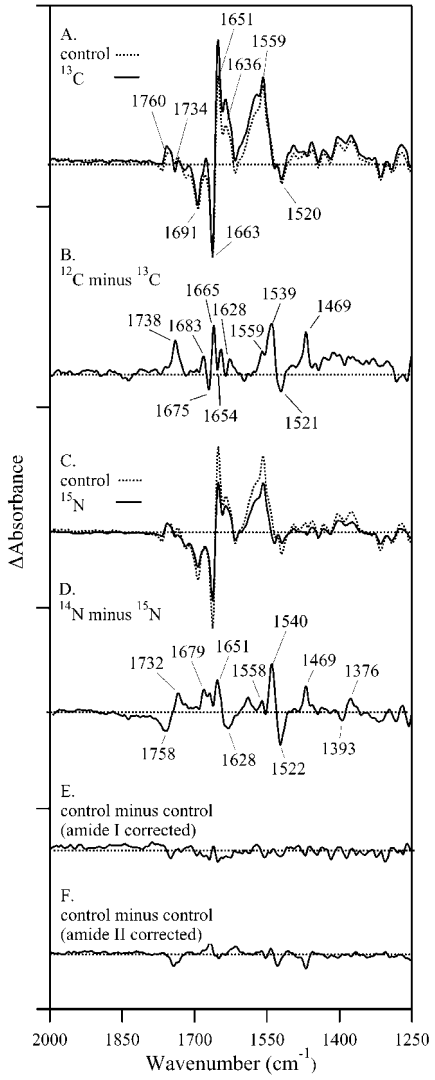

FIGURE 1: Reaction-induced FT-IR spectra associated with the effects of the H^+ electrochemical gradient on the lactose permease. For the control spectra shown in (A), dotted line, and repeated in (C), dotted line, the permease was produced on natural abundance carbon and nitrogen sources. In (A), solid line, the permease was globally ^{13}C labeled by production on [^{13}C]glucose. In (C), solid line, the permease was globally ^{15}N labeled by production on [^{15}N]-ammonium chloride. Spectrum B shows the ^{13}C isotope-edited double difference spectrum [(A), solid line, minus (A), dotted line], and spectrum D shows the ^{15}N isotope-edited double difference spectrum [(C), solid line, minus (C), dotted line]. (B) and (D) are multiplied by a factor of 4 for clarity. A total of 270 difference spectra were acquired from 9 control samples, 180 difference spectra were acquired from 6 ^{13}C samples, and 480 difference spectra were acquired from 16 ^{15}N samples. Spectra averaged to give (A), solid and dashed lines, were amide II normalized and corrected for the 280/565 nm ratio, and then bacteriorhodopsin contributions were subtracted by method I (see Materials and Methods). Spectra averaged to give (C), solid and dashed lines, were amide I normalized and corrected for the 280/565 nm ratio, and then bacteriorhodopsin contributions were subtracted by method I (see Materials and Methods). This difference in correction method was necessary because isotope shifts in the amide I/II absorption bands occurred. Data in (E) and (F) show negative controls for the isotope-edited spectra; these controls were generated by subtraction of one-half of the control data from the other half of the data set. In (E), the control data were normalized by the amide I absorbance before correction for the 280/565 nm ratio. In (F), the control data were normalized by the amide II absorbance before correction for the 280/565 nm ratio. The tick marks on the *y*-axis correspond to 0.005 Δ*A* unit. Other spectral conditions are described in the Materials and Methods section.

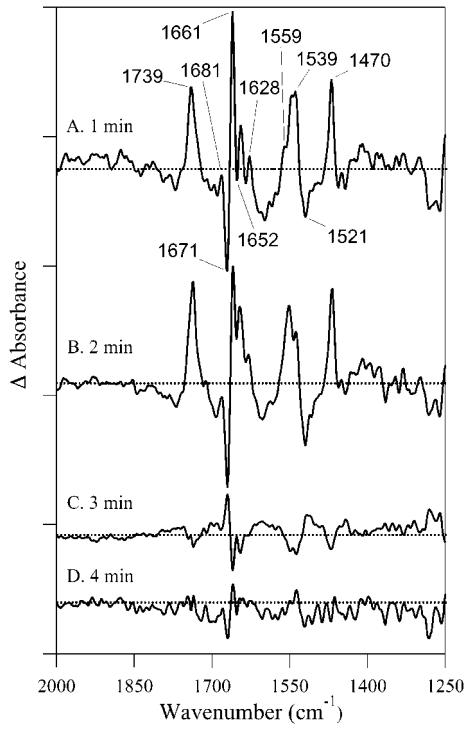

FIGURE 2: Temporal decay of the ^{13}C isotope-edited permease spectra. The permease was natural abundance ^{12}C or ^{13}C labeled, and data correspond to a ^{13}C minus ^{12}C spectrum. In each panel, (A), (B), (C), and (D) were generated from data acquired in the first, second, third, and fourth minute following photoexcitation, respectively. Bacteriorhodopsin contributions were subtracted by method II (Materials and Methods). The tick marks on the *y*-axis represent 0.0005 Δ*A* unit. Other spectral conditions are described in the legend of Figure 1 or the Materials and Methods section.

possibility was presented previously (*20*). Again, bacteriorhodopsin is not labeled in the experiments presented here, so any bacteriorhodopsin contribution will cancel in the isotope-edited data, which will exhibit only permease vibrational bands.

In the data shown in Figure 1, the bacteriorhodopsin contributions were subtracted by method I. Figures 2 and 3 show isotope-edited spectra that were constructed by method II (Materials and Methods) on ^{13}C- and ^{15}N-containing samples, respectively. As expected, both methods of subtraction gave similar results. For example, in the case of the ^{13}C isotope-edited spectrum (Figure 2A), a positive band at 1738 cm^{-1} and bands in the 1540−1520 cm^{-1} region dominate the ^{13}C isotope-edited spectrum. Vibrational bands are also observed in the amide I region (1690−1660, 1640−1620 cm^{-1}), and a positive band is seen at 1470/69 cm^{-1}. The ^{15}N isotope-edited spectra constructed by the two subtraction methods (Figures 3A and 1D) were also similar.

As an additional control, spectral decay was monitored as a function of time. In Figures 2 and 3, spectra were obtained in the first minute (A), the second minute (B), the third minute (C), and the fourth minute (D), after photoexcitation. Inspection of Figures 2 and 3 confirms that changes induced by the gradient decay after laser illumination. Although there was no significant decrease in amplitude in the second minute after photoexcitation (Figures 2B and 3B), by the third time point (Figures 2C and 3C) substantial decreases in amplitude had occurred. Spectral decay was complete 4 min after photoexcitation (Figures 2D and 3D).

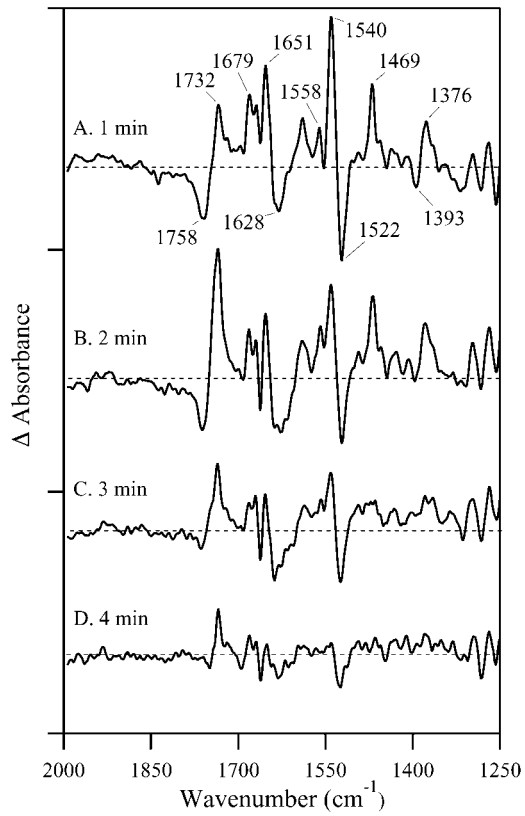

FIGURE 3: Temporal decay of the ^{15}N isotope-edited permease spectra. The permease was natural abundance ^{14}N or ^{15}N labeled, and data correspond to a ^{15}N minus ^{14}N spectrum. In each panel, (A), (B), (C), and (D) were generated from data acquired in the first, second, third, and fourth minute following photoexcitation, respectively. Bacteriorhodopsin contributions were subtracted by method II (Materials and Methods). The tick marks on the *y*-axis represent 0.0005 Δ*A* unit. Other spectral conditions are described in the legend of Figure 1 or the Materials and Methods section.

Note that Figures 2D and 3D give an independent assessment of the uncertainty in these measurements.

DISCUSSION

Ionizable residues on transmembrane segments within the lactose permease have been implicated to play a central or an auxiliary role in the mechanism of H^+/lactose coupling (*13*, *14*, *18*, *26*−*28*). Models from two laboratories have been proposed that describe the sequential steps in the coupling mechanism (*15*, *29*, *30*). While the models differ in their details, the central tenet of both is that H^+/lactose coupling involves a sequence of ionic interactions involving several charged residues. Depending on the model, these residues are Asp-240, Glu-269, Arg-302, Lys-319, His-322, and Glu-325. In addition, Glu-126 and Arg-144 have been postulated to form an essential salt bridge that plays a role in sugar recognition (*31*, *32*).

Nonionizable substitutions at positions 240, 269, 302, 319, and 322 have been shown previously to catalyze H^+/lactose symport, indicating that they are not absolutely required for H^+ binding or transport (*14*, *15*, *18*, *26*−*28*). Single, nonionizable substitutions at Glu-325 catalyzed normal exchange of lactose but were almost completely defective in unidirectional transport (*13*, *14*). Due to the very low rate of net transport, these previous studies did not definitively determine if Glu-325 substitutions can catalyze net H^+ transport. However, the efflux reaction appeared pH insensitive; this result suggests that Glu-325 mutations were unable to recognize H^+ ions (*14*). In recent studies, however, it was found that multiple mutants involving Glu-325 (e.g., K319N/E325Q and K319N/H322Q/E325Q) were able to transport H^+ ions with sugar, indicating that an acidic residue at position 325 is not obligatorily required for H^+ transport in these mutants (*15*, *16*). In these mutants, H^+ ions may follow an alternate path. Alternatively, hydronium ions, rather than H^+ ions as previously presumed, may be the transported species (see ref *16* for a discussion). In any case, the complexity of ionic interactions means that mutagenesis studies alone will not provide a clear picture of the permease coupling mechanism.

To this end, biophysical methods to directly monitor ionization states and ionic interactions within the permease are needed. The FT-IR work presented here is an example. In our previous work, we made tentative assignments of vibrational features to the lactose permease (*20*). In this study, we have used ^{13}C and ^{15}N labeling of the lactose permease to demonstrate the validity of our experimental approach and to make assignments (discussed below). Because FT-IR spectroscopy is sensitive to isotopic substitution, we expect to observe changes in the permease vibrational modes, if the vibrational displacement involves motion of carbon (e.g., C−H, C═O, C−N vibrations) or nitrogen (e.g., C−N, N−H vibrations).

Carboxylic Acid C═O Region. In the 1750−1720 cm^{-1} region, the only expected fundamental vibrational modes in proteins arise from the carbonyl stretching vibration of glutamic and aspartic acid residues (*23*, *24*, *33*). Bands are observed in the permease spectrum in this region (Figure 1A, dotted line). The C═O stretch of carboxylic acid side chains will be ^{13}C sensitive but ^{15}N insensitive. The ^{13}C isotope-edited spectrum (Figures 1B and 2A) exhibits a positive band at 1738/9 cm^{-1} and provides evidence that this vibrational mode involves carbon displacement. This ^{13}C isotope-induced downshift of the 1738/9 cm^{-1} band adds support to the assignment to a C═O stretching vibration of a carboxylic acid side chain. If the C═O assignment is correct, there should be no downshift upon ^{15}N labeling. As additional support for the C═O assignment, the ^{15}N isotope-edited spectrum is observed to be dissimilar in this region (Figures 1D and 3A) and exhibits a negative 1758 cm^{-1} and a positive 1732 cm^{-1} band. This pattern is consistent with a ^{15}N-induced downshift ($\Delta = 26$ cm^{-1}) of a negative band at 1758 cm^{-1}.

However, the ^{13}C downshifted band, which should be observed as a negative band in the ^{13}C isotope-edited spectrum, is not resolved in Figure 1B. A similar observation has been made previously in studies of the effects of ^{13}C labeling on aspartic acid in solution (*34*). We tentatively assign the 1738 cm^{-1} band to the C═O of an aspartic acid or glutamic acid residue.

There are two reasons why a carboxylic acid may contribute to the permease spectrum (reviewed in ref *35*). A carboxylate side chain may protonate when an electrochemical gradient is applied, or an environmental change, such as a change in dielectric constant or hydrogen bonding, may perturb the C═O stretching frequency of the carboxylic acid side chain. When carboxylic acids are perturbed by an environmental change, a derivative-shaped band is expected

in the 1750−1720 cm^{-1} region. Substantial frequency shifts of such a band would give rise to a pattern of two positive and negative lines in the isotope-edited spectrum. Such spectral features are not observed in Figure 1B. When carboxylates are perturbed by a protonation reaction, ^{13}C isotope-sensitive bands, arising from the asymmetric and symmetric stretch of the anion, should be observed in the 1550 and 1375 cm^{-1} region (*34*, *35*). In our data, these bands would be negative, and each band would be accompanied by an isotope-edited component. These bands are not resolved in the isotope-edited data (Figure 1B); however, these are congested spectral regions. In the future, experiments with site-directed mutants will give more information about the perturbation mechanism.

Amide I and Amide II Regions. In the 1680−1620 cm^{-1} region, amide I vibrational bands are expected (*36*). Amide side chain (i.e., glutamine and asparagine) vibrations may also contribute a minor amount of intensity in this spectral region (*24*, *37*). The amide I vibration arises from a predominantly C═O stretching mode (*36*) and is thus expected to be ^{13}C sensitive. ^{13}C-induced downshifts of 40−50 cm^{-1} have been measured previously (*21*, *38*, *39*). In our data (Figures 1B and 2A), ^{13}C-sensitive spectral features are observed in the isotope-edited spectrum at (positive) 1683/1, (negative) 1675/1, and (positive) 1628 cm^{-1}. (As stated above, the region between 1660 and 1640 cm^{-1} is not interpretable in the difference spectrum.) The observed interpretable bands in the isotope-edited spectrum have frequencies that are characteristic of the amide I vibration from the peptide bond (*37*).

The amide I vibration is also expected to be weakly ^{15}N sensitive with predicted ^{15}N isotope shifts of <4 cm^{-1} (*40*). In agreement with this expectation, the ^{15}N isotope-edited permease spectrum exhibited spectral bands in the amide I region, but with altered frequencies and amplitudes, when compared to the ^{13}C isotope-edited spectrum. This is expected if the vibrational contributors are amide I modes, because the magnitude of the ^{13}C and ^{15}N isotope shifts are different. Also consistent with an amide I assignment for the 1680−1630 cm^{-1} region, a ^{13}C- and ^{15}N-sensitive band is observed at 1559/8 cm^{-1} (*40*, *36*, *41*). Taken together, the ^{13}C- and ^{15}N-labeling experiments support an amide I assignment for the (positive) 1683/1, (negative) 1675/1, and (positive) 1628 cm^{-1} bands and an amide II assignment for the (positive) 1559/8 cm^{-1} band.

The amide I frequencies (∼1680 and ∼1630 cm^{-1}) observed in the ^{13}C and ^{15}N isotope-edited permease spectra are characteristic of β-strands and turns in proteins (*42*). This is of interest because FT-IR studies of this lactose permease preparation have shown that it is predominantly ∼80% α-helical, with the rest of the spectrum assigned to turns (*10*). However, that previous result is not in contradiction to this work. The amplitudes of the bands observed here are on the order of 10^{-4} absorbance units and correspond to localized changes in secondary structure, which would not be observable without the use of reaction-induced techniques.

Multiple positive and negative bands in the ^{13}C isotope-edited spectrum indicate that several components of the amide vibration are perturbed upon isotopic labeling. One possible explanation of these results is that individual secondary structure components, such as turns or β-sheet, may interconvert. Alternatively, a change in the strength of hydrogen bonding may occur when the H^+ electrochemical gradient is applied. Finally, changes in conformation and orientation can lead to changes in transition dipole coupling, and such changes may alter the amide I spectrum.

Other Spectral Regions. ^{13}C- and ^{15}N-sensitive bands at (positive) ∼1540, (negative) ∼1520, and (positive) ∼1469 cm^{-1} are found in common between the two isotope-edited spectra. This pattern can arise from the downshift of a derivative-shaped spectral feature. This result suggests that these bands arise from vibrational modes for which the ^{13}C and ^{15}N isotope shifts are similar. Possible origins are CN vibrational modes in lysine, arginine, histidine, glutamine, and/or asparagine (*23*, *24*, *36*, *43*).

The ^{15}N isotope-edited spectrum (Figures 1D and 3A) shows two spectral features that are not resolved in the ^{13}C spectrum: a derivative-shaped feature at (negative) 1393 and (positive) 1376 cm^{-1}. The ^{13}C isotope-edited spectrum exhibits only weak, positive intensity in the 1400 cm^{-1} region. These vibrational bands may correspond to NH deformation modes of a nitrogen-containing amino acid side chain.

Lysine, arginine, and histidine residues (e.g., R144, R302, K319, and H322) in the permease have been implicated previously as important for transport function (reviewed in refs *11* and *12*). Definitive identification of these spectral features will be performed by more specific labeling experiments and site-directed mutagenesis.

Summary. The ^{13}C- and ^{15}N-labeling studies presented here provide support for the conclusion that the electrochemical gradient causes a change in permease structure. There are three identified components to this structural change. First, a change in the peptide backbone occurs. This may be an interconversion of secondary structural elements, a change in helix placement, or a change in hydrogen bond strength. Second, evidence for a gradient-induced environmental or protonation change in a carboxylic acid residue has been presented. Third, perturbation of a nitrogen-containing side chain has been observed. These structural changes could play a role in storage of free energy from the gradient or in changing the affinity for the co-substrate, lactose (*44*). The observation that the permease undergoes a change in secondary structure upon imposition of the electrochemical gradient may have important ramifications for structural changes during transport (*45*). Because either the electric potential or the proton gradient can drive the transport process, the secondary structure change may be driven either by a direct protonation reaction or by an electric field-induced helix shift.

In the experiments described here, lactose has been omitted from the sample. The imposition of an H^+ electrochemical gradient will result in structural changes associated with H^+ binding. However, since the permease is obligatorily coupled, other conformational changes associated with the transport process will not occur in the absence of lactose. In future experiments, structural changes associated with lactose transport will be probed.

ACKNOWLEDGMENT

The authors thank Prof. Roseann Sachs, Mr. T. Krick, and the Mass Spectrometry Consortium for the Life Sciences for assistance with the GC/MS experiments.

REFERENCES

1. Cohen, G. N., and Monod, J. (1957) *Bacterial. Rev. 21*, 169−194.
2. Pao, S. S., Paulsen, I. T., and M. J. Saier, J. (1998) *Microbiol. Mol. Biol. Rev. 62*, 1−34.
3. West, I. C., and Mitchell, P. (1973) *Biochem. J. 132*, 587−592.
4. Teather, R. M., Müller-Hill, B., Abrutsch, U., Aichele, G., and Overath, P. (1978) *Mol. Gen. Genet. 159*, 239−248.
5. Buchel, D. E., Gronenborn, B., and Müller-Hill, B. (1980) *Nature 283*, 541−545.
6. Mieschendahl, M., Buchel, D., Bocklage, H., and Muller-Hill, B. (1981) *Proc. Natl. Acad. Sci. U.S.A. 78*, 7652−7656.
7. Foster, D. L., Boublik, M., and Kaback, H. R. (1983) *J. Biol. Chem. 258*, 31−34.
8. Calamia, J., and Manoil, C. (1990) *Proc. Natl. Acad. Sci. U.S.A. 87*, 4937−4941.
9. Le Coutre, J., Narasimhan, L. R., Patel, C. K., and Kaback, H. R. (1997) *Proc. Natl. Acad. Sci. U.S.A. 94*, 10167−10171.
10. Patzlaff, J. S., Moeller, J. A., Barry, B. A., and Brooker, R. J. (1998) *Biochemistry 37*, 15363−15375.
11. Varela, M. F., and Wilson, T. H. (1996) *Biochim. Biophys. Acta 1276*, 21−34.
12. Kaback, H. R., and Wu, J. (1999) *Acc. Chem. Res. 32*, 805−813.
13. Carrasco, N., Puttner, I. B., Antes, L. M., Lee, J. A., Larigan, J. D., Lolkema, J. S., Roepe, P. D., and Kaback, H. R. (1989) *Biochemistry 28*, 2533−2539.
14. Franco, P. J., and Brooker, R. J. (1994) *J. Biol. Chem. 269*, 7379−7386.
15. Johnson, J. L., and Brooker, R. J. (1999) *J. Biol. Chem. 274*, 4074−4081.
16. Johnson, J. L., Lockheart, M. S. K., and Brooker, R. J. (2001) *J. Membr. Biol. 181*, 215−224.
17. Voss, J., Hubbell, W. L., and Kaback, H. R. (1995) *Proc. Natl. Acad. Sci. U.S.A. 92*, 12300−12303.
18. He, M. M., Voss, J., Hubbell, W., and Kaback, H. R. (1995) *Biochemistry 34*, 15667−15670.
19. He, M. M., Voss, J., Hubbell, W. L., and Kaback, H. R. (1995) *Biochemistry 34*, 15661−15666.
20. Patzlaff, J. S., Brooker, R. J., and Barry, B. A. (2000) *J. Biol. Chem. 275*, 28695−28700.
21. Hutchison, R. S., Betts, S. D., Yocum, C. F., and Barry, B. A. (1998) *Biochemistry 37*, 5643−5653.
22. Patterson, B. W., Carraro, F., and Wolfe, R. R. (1993) *Biol. Mass Spectrom. 22*, 518−523.
23. Venyaminov, S. Y., and Kalnin, N. N. (1990) *Biopolymers 30*, 1243−1257.
24. Rahmelow, K., Hubner, W., and Achermann, T. (1998) *Anal. Biochem. 257*, 1−11.
25. Hermansson, K., and Tepper, H. (1996) *Mol. Phys. 89*, 1291−1299.
26. Brooker, R. J. (1991) *J. Biol. Chem. 266*, 4131−4138.
27. Lee, J. I., Hwang, P. P., and Wilson, T. H. (1993) *J. Biol. Chem. 268*, 20007−20015.
28. Ujwal, M. L., Sahin-Tóth, M., Persson, B., and Kaback, H. R. (1994) *Mol. Membr. Biol. 11*, 9−16.
29. Kaback, H. R. (1997) *Proc. Natl. Acad. Sci. U.S.A. 94*, 5539−5543.
30. Sahin-Tóth, M., Karlin, A., and Kaback, H. R. (2000) *Proc. Natl. Acad. Sci. U.S.A. 97*, 10729−10732.
31. Frillingos, S., Gonzalez, A., and Kaback, H. R. (1997) *Biochemistry 36*, 14284−14290.
32. Sahin-Tóth, M., le Coutre, J., Kharabi, D., le Maire, G., Lee, J. C., and Kaback, H. R. (1999) *Biochemistry 38*, 813−819.
33. Ramirez, F. J., and Navarrete, J. T. L. (1995) *Spectrochim. Acta 51A*, 293−302.
34. Hutchison, R. S., Steenhuis, J. J., Yocum, C. F., Razeghifard, R. M., and Barry, B. A. (1999) *J. Biol. Chem. 274*, 31987−31995.
35. Steenhuis, J. J., and Barry, B. A. (1997) *J. Phys. Chem. B 101*, 6652−6660.
36. Krimm, S., and Bandekar, J. (1986) in *Advances in Protein Chemistry* (Anfinsen, C. B., Edsall, J. T., and Richards, F. M., Eds.) pp 181−364, Academic Press, New York.
37. Bellamy, L. J. (1980) *The infrared spectra of complex molecules*, Vol. II, Chapman and Hall, London.
38. Haris, P. I., Robillard, G. T., Van Dijk, A. A., and Chapman, D. (1992) *Biochemistry 31*, 6279−6284.
39. Zhang, M., Fabian, H., Mantsch, H. H., and Vogel, H. J. (1994) *Biochemistry 33*, 10883−10888.
40. Balazs, A. (1981) *Acta Chim. Acad. Sci. Hung. 109*, 265−285.
41. Bernard, M. T., MacDonald, G. M., Nguyen, A. P., Debus, R. J., and Barry, B. A. (1995) *J. Biol. Chem. 270*, 1589−1594.
42. Surewicz, W. K., Mantsch, H. A., and Chapman, D. (1993) *Biochemistry 32*, 389−394.
43. MacDonald, G. M., and Barry, B. A. (1992) *Biochemistry 31*, 9848−9856.
44. Kaczorowski, G. J., Robertson, D. E., and Kaback, H. R. (1979) *Biochemistry 18*, 3697−3704.
45. Green, A. L., Anderson, E. J., and Brooker, R. J. (2000) *J. Biol. Chem. 275*, 23240−23246.

BI025555G